Transmit Subaperturing for MIMO Radars With Co-Located Antennas

Hongbin Li, *Senior Member, IEEE*, and Braham Himed, *Fellow, IEEE*

***Abstract*—We present a transmit subaperturing (TS) approach for multiple-input multiple-output (MIMO) radars with co-located antennas. The proposed scheme divides the transmit array elements into multiple groups, each group forms a directional beam and modulates a distinct waveform, and all beams are steerable and point to the same direction. The resulting system is referred to as a TS-MIMO radar. A TS-MIMO radar is a tunable system that offers a continuum of operating modes from the phased-array radar, which achieves the maximum directional gain but the least interference rejection ability, to the omnidirectional transmission based MIMO radar, which can handle the largest number of interference sources but offers no directional gain. Tuning of the TS-MIMO system can be easily made by changing the configuration of the transmit subapertures, which provides a direct tradeoff between the directional gain and interference rejection power of the system. The performance of the TS-MIMO radar is examined in terms of the output signal-to-interference-plus-noise ratio (SINR) of an adaptive beamformer in an interference and training limited environment, where we show analytically how the output SINR is affected by several key design parameters, including the size/number of the subapertures and the number of training signals. Our results are verified by computer simulation and comparisons are made among various operating modes of the proposed TS-MIMO system.**

***Index Terms*—Adaptive processing for multiple-input multiple-output (MIMO) radars, MIMO radars, subaperture, transmit beamforming.**

I. Introduction

PHASED arrays consisting of multiple closely spaced array elements have been widely used in many modern radar systems [1]. A standard phased-array radar can be considered as a single-input multiple-output (SIMO) system, where a probing waveform is radiated via an electronically steerable transmit beam and the returned signal is collected via multiple receive array elements. The transmit beam is formed by having each of the radiating elements transmit a phase-shifted version of the same probing waveform. It offers a directional gain which is useful for detecting/tracking weak targets in the radar look direction while suppressing strong sidelobe interferences from other directions.

A different strategy is to employ multiple distinct probing waveforms. These waveforms can be radiated from a transmit array and separated at the receive array via a set of matched filters. This effectively leads to a multiple-input multiple-output (MIMO) radar system, which has received a lot of interest in recent years (see [2], [3] and references therein). MIMO radars offer unique advantages over their phased-array counterparts. For example, with adequately separated transmit/receive array elements, an MIMO radar can probe a fluctuating target from different aspect angles, which offers a detection diversity gain [3], [4]. An MIMO radar can provide higher spatial resolution and degrees of freedom (DoFs) [5], better parameter identifiability [6], and allow direct application of adaptive array techniques [7]. Many of such capabilities are fundamentally due to the fact that an MIMO radar realizes a virtual or effective aperture that is larger than the physical receive array of its phased-array counterpart [8].

A standard MIMO radar takes the opposite direction of the phased-array radar [9]. The approach is to employ multiple uncorrelated waveforms that are radiated via omnidirectional transmission, in contrast to a phased-array radar where a single probing waveform is sent via directional transmission. While an omni-MIMO radar retains the benefits discussed above over a phased-array radar, the former misses the directional gain and spatial selectivity induced by directional transmission. Intermediates between the two extremes were considered by using correlated waveforms and transmit beamforming [9], [10]. The objective was to determine a correlation matrix of the probing waveforms. The problem was formulated as a constrained optimization, along with a preselected transmit beampattern, or a set of desired attributes of the transmit beampattern. The solution generally cannot be obtained in closed-form and requires sophisticated optimization techniques. The resulting waveforms are usually complicated, not having a constant envelope, and may be difficult for synthesis and power amplification.

In this paper, we propose a simple transmit subaperturing (TS) approach for MIMO radars with co-located antennas, and the resulting system is called a TS-MIMO radar for brevity. The main idea is to form multiple transmit subapertures, by dividing the total number of transmit array elements into multiple groups, which may be disjoint or overlapping in space. Each transmit subaperture forms a directional beam and carries a distinct waveform, and all transmit beams are steered toward the same direction. The returned signal is collected using a receive array and the waveforms are separated via a matched filter, like the omni-MIMO radar.

The proposed TS-MIMO radar is a tunable systems that offers a continuum of operating modes ranging from the phased-array radar to the omni-MIMO radar. Tuning is achieved by changing the size and number of the transmit subapertures. We show that

Manuscript received February 02, 2009; revised August 11, 2009. Current version published January 20, 2010. This work was supported in part by the Air Force Research Laboratory (AFRL) under Contract FA8750-05-2-0001 and in part by the Air Force Office of Scientific Research (AFOSR) under Grant FA9550-09-1-0310. The associate editor coordinating the review of this manuscript and approving it for publication was Prof. Rick S. Blum.

H. Li is with the Department of Electrical and Computer Engineering, Stevens Institute of Technology, Hoboken, NJ 07030 USA (e-mail: hongbin.li@stevens.edu).

B. Himed is with the AFRL/RYRT, 2241 Avionics Circle, Dayton, OH 45433 USA (e-mail: braham.himed@wpafb.af.mil).

Color versions of one or more of the figures in this paper are available online at http://ieeexplore.ieee.org.

Digital Object Identifier 10.1109/JSTSP.2009.2038967

by so doing there is a direct trade-off between the directional gain and interference rejection capability achieved by a specific combination. The performance of the proposed TS-MIMO system is examined in an interference limited environment with multiple spatially distributed interferers. The performance metric is the output signal-to-interference-plus-noise ratio (SINR) of an adaptive beamformer, namely the minimum-variance distortionless-response (MVDR) or Capon beamformer [11], [12], and its beampattern. We obtain closed-form expressions of the distribution, mean and variance of the output SINR, which are useful to analyze the performance of the TS-MIMO system at various operating modes (including the phased-array and omni-MIMO modes) in interference and training limited scenarios. By training limited, it is meant that the number of training data available for adaptive processing in the real world is limited. We show that the output SINR is directly impacted by several key design parameters of the TS-MIMO radar, including the number and size of the transmit subapertures as well as the number of training signals.

The remainder of the paper is organized as follows. In Section II, we provide an overview of the conventional phased-array and omni-MIMO radars. The proposed TS-MIMO system is presented in Section III, along with discussions on several relevant issues. Adaptive beamforming and SINR analysis for the three radar systems are considered in Section IV. Numerical results are included in Section V, followed by conclusions in Section VI.

II. Standard Phased-Array and MIMO Radars

In this section, we provide an overview of the conventional phased-array radar and MIMO radar. We introduce necessary symbols and equations to facilitate the comparison of these existing and our proposed approaches.

Notation: Vectors (matrices) are denoted by boldface lower (upper) case letters, all vectors are column vectors, superscripts $(\cdot)^*$, $(\cdot)^T$, and $(\cdot)^H$ denote complex conjugate, transpose, and complex conjugate transpose, respectively, $E\{\cdot\}$ denotes statistical expectation, $\mathbf{I}$ denotes an identity matrix, $\otimes$ denotes the Kronecker product, and $\mathrm{vec}(\cdot)$ denotes the operation of stacking the columns of a matrix on top of each other.

A. Phased-Array Radar

Consider a phased-array radar with N_t co-located transmit elements and N_r co-located receive elements. As illustrated in Fig. 1(a), a phased-array radar typically employs one transmit aperture consisting of all N_t transmit elements forming a directional transmit beam that points toward some look direction θ_0. Directional transmission is achieved by having each of the N_t elements transmitting a phase-shifted version of a waveform $s(l), l = 1, 2, \ldots, L$, where L denotes the number of samples of each transmitted pulse [1]. Specifically, the baseband equivalent model, in complex-valued form, of the transmitted signals from the N_t transmit elements can be expressed as

$$\mathbf{a}_t^*(\theta_0)s(l), \quad l = 1, 2, \ldots, L \tag{1}$$

where $\mathbf{a}_t(\theta_0)$ denotes the $N_t \times 1$ transmit steering vector containing complex-valued elements with unit amplitude and phase determined by the look angle θ_0 [1]. As an example, for a uniform linear array (ULA) with a half-wavelength separation between two adjacent array elements, the steering vector is given by [13, Ch.6]

$$\mathbf{a}_t(\theta) = \left[\, 1 \quad e^{-j\pi\sin\theta} \quad \ldots \quad e^{-j(N_t-1)\pi\sin\theta} \,\right]^T. \tag{2}$$

The signal seen at a specific location with angle θ_i in the far field is a superposition of the delayed and attenuated version of the transmitted signals. Throughout this paper, we assume a narrowband system where the propagation delays manifest as phase shifts to the transmitted signals, such that the signal seen at that location is given by [13, Ch.6] (also see [2])

$$\mathbf{a}_t^T(\theta_i)\mathbf{a}_t^*(\theta_0)s(l) \triangleq \beta_i s(l) \tag{3}$$

where the first $\mathbf{a}_t(\theta_i)$ on the left side is a propagation vector due to propagation effects, and takes the same form of the steering vector. For notational simplicity and following the convention of many existing works in array signal processing (e.g., [2], [4], [8], [14] and references therein), both are simply referred to as the steering vector hereafter.

It follows that the signal seen at the look angle θ_0 is given by

$$\mathbf{a}_t^T(\theta_0)\mathbf{a}_t^*(\theta_0)s(l) = N_t s(l) \tag{4}$$

where we see a *directional gain* of N_t (the size of the transmit aperture) at the look direction, which is a well-known property of phased-array radars. Since $|\beta_i| \leq N_t$ for $\theta_i \neq \theta_0$, the directional gain is useful in mitigating sidelobe interference.

Suppose there is a target located at the look direction θ_0 along with multiple interference sources located at $\theta_i \neq \theta_0$. The baseband equivalent of the signals at the receive array, $\mathbf{x}_{\mathrm{pa}}(l)$, $l = 1, 2, \ldots, L$, where the subscripts stand for phased-array, are given by

$$\begin{aligned}\mathbf{x}_{\mathrm{pa}}(l) &= \alpha_0\mathbf{a}_r(\theta_0)\mathbf{a}_t^T(\theta_0)\mathbf{a}_t^*(\theta_0)s(l) \\ &\quad + \sum_i \alpha_i\mathbf{a}_r(\theta_i)\mathbf{a}_t^T(\theta_i)\mathbf{a}_t^*(\theta_0)s(l) + \mathbf{n}(l) \\ &= \alpha_0 N_t\mathbf{a}_r(\theta_0)s(l) + \sum_i \alpha_i\beta_i\mathbf{a}_r(\theta_i)s(l) + \mathbf{n}(l)\end{aligned} \tag{5}$$

where α_i denotes the complex amplitude of the ith source, $\mathbf{a}_r(\theta)$ an $N_r \times 1$ propagation vector due to the propagation delays from a source to the receive elements, and $\mathbf{n}(l)$ the $N_r \times 1$ additive white Gaussian noise vector with zero mean and covariance matrix $\sigma_n^2\mathbf{I}$. The vector $\mathbf{a}_r(\theta)$, which is similarly defined as the transmit steering vector $\mathbf{a}_t(\theta)$, is usually referred to as the receive steering vector [14]. Note that when the transmit and receive arrays are not co-located, the look and receive angles are different. However, since the relative positions of the two arrays are typically known, the same directional variable θ is used for notational convenience (also see [6]).

The received signal is processed by a matched filter, which outputs

$$\mathbf{y}_{\mathrm{pa}} \triangleq \frac{\sum_{l=1}^{L} \mathbf{x}_{\mathrm{pa}}(l)s^*(l)}{\sum_{l=1}^{L} |s(l)|^2}$$

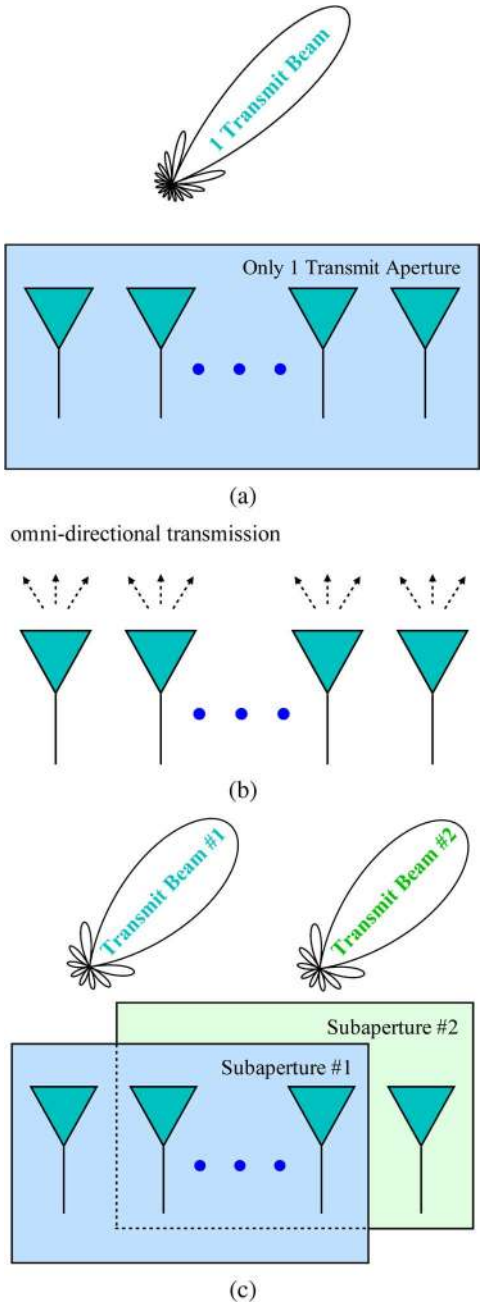

Fig. 1. Transmit array configurations of three radar systems. (a) Phased-array radar with one transmit aperture and directional transmission. (b) Standard omni-MIMO radar with omnidirectional transmission. (c) Proposed TS-MIMO radar with multiple transmit subapertures (two subapertures shown) and directional transmission.

$$= \alpha_0 N_t \mathbf{a}_r(\theta_0) + \sum_i \alpha_i \beta_i \mathbf{a}_r(\theta_i) + \frac{\sum_{l=1}^{L} \mathbf{n}_{\rm pa}(l) s^*(l)}{\sum_{l=1}^{L} |s(l)|^2} \triangleq \alpha_0 \mathbf{a}_{\rm pa}(\theta_0) + \sum_i \alpha_i \mathbf{a}_{\rm pa}(\theta_i) + \mathbf{n}_{\rm pa} \quad (6)$$

where the scaled steering vector

$$\mathbf{a}_{\rm pa}(\theta_i) \triangleq \beta_i \mathbf{a}_r(\theta_i) \quad (7)$$

is introduced to unify the analysis in Section IV. It is easy to verify that $\mathbf{n}_{\rm pa}$ has zero mean and covariance matrix $\sigma_n^2\mathbf{I}$. By assuming that the target/interference complex amplitudes α_i are mutually uncorrelated with zero mean and variance σ_i^2, the interference-plus-noise covariance matrix can be written as

$$\mathbf{R}_{\rm pa} = \sum_i \sigma_i^2 \mathbf{a}_{\rm pa}(\theta_i)\mathbf{a}_{\rm pa}^H(\theta_i) + \sigma_n^2\mathbf{I}. \quad (8)$$

B. MIMO Radar With Omnidirectional Transmission

A standard MIMO radar proposal involves omnidirectional transmission from all transmit elements without forming a directional beam [9]. Such an MIMO radar is henceforth referred to as the omni-MIMO radar. An illustration of the transmit array configuration is shown in Fig. 1(b). Specifically, consider an omni-MIMO radar with N_t co-located transmit elements and N_r co-located receive elements, where each transmit element sends out a different waveform $s_n(l)$, $n = 1, 2, \ldots, N_t$, and $l = 1, 2, \ldots, L$, via omnidirectional transmission. Let $\mathbf{s}(l)$ be the $N_t \times 1$ vector collecting all these waveforms. The signal seen at a location with angle θ is $\mathbf{a}_t^T(\theta)\mathbf{s}(l)$ [2]. The baseband equivalent of the signals received at the N_r-element receive array are given by

$$\mathbf{x}_{\rm od}(l) = \alpha_0 \mathbf{a}_r(\theta_0)\mathbf{a}_t^T(\theta_0)\mathbf{s}(l) + \sum_i \alpha_i \mathbf{a}_r(\theta_i)\mathbf{a}_t^T(\theta_i)\mathbf{s}(l) + \mathbf{n}(l), \quad l = 1, 2, \ldots, L \quad (9)$$

where the symbols are similarly defined as in (5) and the subscripts "od" signifies omnidirectional.

The received signals are again processed by a matched filter, which outputs an $N_r \times N_t$ matrix given by

$$\mathbf{Y}_{\rm od} = \left[\sum_{l=1}^{L} \mathbf{x}_{\rm od}(l)\mathbf{s}^H(l)\right]\left[\sum_{l=1}^{L} \mathbf{s}(l)\mathbf{s}^H(l)\right]^{-1} = \alpha_0 \mathbf{a}_r(\theta_0)\mathbf{a}_t^T(\theta_0) + \sum_i \alpha_i \mathbf{a}_r(\theta_i)\mathbf{a}_t^T(\theta_i) + \mathbf{N}_{\rm od} \quad (10)$$

where

$$\mathbf{N}_{\rm od} \triangleq \left[\sum_{l=1}^{L} \mathbf{n}(l)\mathbf{s}^H(l)\right]\left[\sum_{l=1}^{L} \mathbf{s}(l)\mathbf{s}^H(l)\right]^{-1}. \quad (11)$$

We assume that the transmitted waveforms are orthonormal, i.e., $\sum_{l=1}^{L} \mathbf{s}(l)\mathbf{s}^H(l) = \mathbf{I}$, which is a standard choice to simplify the implementation of the matched filter and reduce its computational complexity. In this case, it is easy to show that $\mathbf{N}_{\rm od}$ contains independent and identically distributed (i.i.d.) Gaussian entries with zero mean and variance σ_n^2. Stacking the columns of $\mathbf{Y}_{\rm od}$ on top of one another leads to

$$\mathbf{y}_{\rm od} \triangleq {\rm vec}(\mathbf{Y}_{\rm od}) = \alpha_0 \mathbf{a}_{\rm od}(\theta_0) + \sum_i \alpha_i \mathbf{a}_{\rm od}(\theta_i) + \mathbf{n}_{\rm od} \quad (12)$$

where $\mathbf{n}_{\rm od} \triangleq \mathrm{vec}(\mathbf{N}_{\rm od})$ and

$$\mathbf{a}_{\rm od}(\theta) \triangleq \mathbf{a}_t(\theta) \otimes \mathbf{a}_r(\theta) \tag{13}$$

denotes the joint transmit-receive steering vector. Unlike the phased-array radar, the omni-MIMO radar provides no directional gain for a target at θ_0. Advantages of the latter include increased DoFs, better spatial resolution, and stronger capability of dealing with interference [2], [6], [8].

Similar to the phase-array radar, the interference-plus-noise covariance matrix for the omni-MIMO radar can be expressed as (also see [8])

$$\mathbf{R}_{\rm od} = \sum_i \sigma_i^2 \mathbf{a}_{\rm od}(\theta_i)\mathbf{a}_{\rm od}^H(\theta_i) + \sigma_n^2 \mathbf{I}. \tag{14}$$

III. MIMO Radar With Transmit Subaperturing

We now consider a new strategy for MIMO radar operation by including transmit subaperturing. We show that the resulting TS-MIMO system subsumes the phased-array and omni-MIMO radar as special cases.

A. TS-MIMO Radar

The general idea of the TS-MIMO radar is to form multiple transmit beams which are steered toward the same direction. This is different from a phased-array radar, which forms a single directional beam, or an omni-MIMO radar, which employs omnidirectional transmission and no directional beam. Multiple transmit beams using an antenna array can be formed by grouping the array elements into multiple groups, each forming a transmit subaperture. These transmit subapertures can be disjoint or overlapping (i.e., with shared array elements) in space, thus offering flexible configuration. An illustration of the transmit array configuration for a TS-MIMO radar with two overlapping transmit subapertures is shown in Fig. 1(c).

As in the earlier cases, we assume that the transmit array has N_t co-located elements whereas the receive array has N_r co-located elements. A total of $M \leq N_t$ transmit subapertures are employed, and the mth transmit aperture contains $N_{t,m}$ array elements. Let $\mathbf{b}_m(\theta)$ denote the steering vector associated with the mth transmit subaperture, which is an $N_{t,m} \times 1$ sub-vector formed from the transmit steering vector $\mathbf{a}_t(\theta)$ for the entire transmit array. An example of the transmit subaperture configuration and the corresponding steering vectors are discussed in Section III-B.

The M transmit subapertures along with their steering vectors $\mathbf{b}_m(\theta)$ are used to form M directional beams, each modulating a different waveform $s_m(l)$, $m = 1,2,\ldots,M$, and $l = 1,2,\ldots,L$. The signal transmitted by the mth subaperture steered toward an angle θ_0 is given by $\mathbf{b}_m^*(\theta_0)s_m(l)$. Clearly, the signals sent out from the array elements within the same subaperture are phased-shifted versions of an identical waveform, just like the phased-array radar. The baseband equivalent of the signal seen at a location with angle θ_i in the far field due to the above transmitted signal is given by

$$\mathbf{b}_m^T(\theta_i)\mathbf{b}_m^*(\theta_0)s_m(l). \tag{15}$$

The overall signal seen at that location is then a superposition of the transmissions from all M subapertures

$$\sum_m \mathbf{b}_m^T(\theta_i)\mathbf{b}_m^*(\theta_0)s_m(l) \triangleq \boldsymbol{\zeta}_i^T \mathbf{s}_M(l) \tag{16}$$

where

$$\mathbf{c}(\theta) \triangleq [\, e^{j\phi_1(\theta)} \quad \ldots \quad e^{j\phi_M(\theta)} \,]^T \tag{17}$$

$$\zeta_{i,m} \triangleq \mathbf{b}_m^T(\theta_i)\mathbf{b}_m^*(\theta_0) \tag{18}$$

$$\boldsymbol{\zeta}_i \triangleq [\, \zeta_{i,1} \quad \ldots \zeta_{i,M} \,]^T \tag{19}$$

$$\mathbf{s}_M(l) \triangleq [\, s_1(l) \quad \ldots \quad s_M(l) \,]^T. \tag{20}$$

With the above discussion, we can now determine the signal at the receive array of a TS-MIMO radar. Suppose that a target is located at angle θ_0 and multiple interference sources at $\{\theta_i\}$. The received signal is given by

$$\mathbf{x}_{\rm ts}(l) = \kappa\alpha_0 \mathbf{a}_r(\theta_0)\boldsymbol{\zeta}_0^T \mathbf{s}_M(l) + \kappa \sum_i \alpha_i \mathbf{a}_r(\theta_i)\boldsymbol{\zeta}_i^T \mathbf{s}_M(l) + \mathbf{n}(l) \tag{21}$$

where the symbols are similarly defined as for the phased-array and omni-MIMO radars, and the subscripts "ts" denotes transmit subaperturing. Note that the nth element of $\mathbf{x}_{\rm ts}(l)$ represents the signal received at the nth antenna of the receive array. Also note that an amplitude scaling parameter κ is introduced in the above equation, which is to ensure the total transmission power of the TS-MIMO radar is the same as that of the phased-array radar or of the omni-MIMO radar for fair comparison. Suppose that for all three radar systems, each waveform contains identically unit energy

$$\sum_l |s_n(l)|^2 = \sum_l |s(l)|^2 = 1, \quad n = 1,2,\ldots,N_t. \tag{22}$$

It is easy to verify that the identical transmission power constraint is met if we choose

$$\kappa = \sqrt{\frac{N_t}{\sum_m N_{t,m}}}. \tag{23}$$

Equation (21) is similar to that for the omni-MIMO radar with one distinction. In particular, observe the directional gain of [cf. (18)]

$$\boldsymbol{\zeta}_0 = [\, N_{t,1} \quad N_{t,2} \quad \ldots \quad N_{t,M} \,]^T \tag{24}$$

at the look direction, offered by transmit subaperturing and directional transmission, which is not present in the omni-MIMO radar.

Next, matched filtering is applied on the received signal, yielding an $N_r \times M$ matrix (assuming orthonormal waveforms)

$$\mathbf{Y}_{\rm ts} \triangleq \sum_{l=1}^{L} \mathbf{x}_{\rm ts}(l)\mathbf{s}_M^H(l) = \kappa\alpha_0 \mathbf{a}_r(\theta_0)\boldsymbol{\zeta}_0^T + \kappa \sum_i \alpha_i \mathbf{a}_r(\theta_i)\boldsymbol{\zeta}_i^T + \mathbf{N}_{\rm ts} \tag{25}$$

where $\mathbf{N}_{\rm ts} \triangleq \sum_{l=1}^{L} \mathbf{n}(l)\mathbf{s}_M^H(l)$. Stacking the columns of the matrices on top of each other gives

$$\mathbf{y}_{\rm ts} = \alpha_0 \mathbf{a}_{\rm ts}(\theta_0) + \sum_i \alpha_i \mathbf{a}_{\rm ts}(\theta_i) + \mathbf{n}_{\rm ts} \tag{26}$$

where

$$\mathbf{a}_{\rm ts}(\theta_i) = \kappa \boldsymbol{\zeta}_i \otimes \mathbf{a}_r(\theta_i). \tag{27}$$

Under the same conditions as stated for the phased-array and omni-MIMO radars, the interference-plus-noise covariance matrix for the TS-MIMO radar is given by

$$\mathbf{R}_{\rm ts} = \sum_i \sigma_i^2 \mathbf{a}_{\rm ts}(\theta_i)\mathbf{a}_{\rm ts}^H(\theta_i) + \sigma_n^2 \mathbf{I}. \tag{28}$$

B. Example

We consider one illustrating example where the transmitter and receiver share a ULA of $N_t = N_r = N$ elements. Suppose M equal-sized transmit subapertures are to be formed. Overlapping is employed to maximize the size of each subaperture and, in turn, its associated directional gain. Specifically, let

$$L \triangleq N - M + 1 \tag{29}$$

which is the largest subaperture size for fixed N and M. The first subaperture is formed by antenna elements 1 to L, the second by 2 to $L+1$, and the last by $N-L+1$ to N. On the other hand, the receive array employs a single aperture consisting of all N array elements. Assume that the inter-element spacing of the ULA is half wavelength. The transmit and receive steering vectors are identically given by [13, Ch.6]

$$\mathbf{a}(\theta) = [\,1 \quad e^{-j\pi\sin\theta} \quad \ldots \quad e^{-j(N-1)\pi\sin\theta}\,]^T. \tag{30}$$

The steering vector for the mth transmit subaperture is given by an $L \times 1$ subvector of $\mathbf{a}(\theta)$:

$$\mathbf{b}_m(\theta) = [\,e^{-j(m-1)\pi\sin\theta} \quad \ldots \quad e^{-j(m+L-2)\pi\sin\theta}\,]^T. \tag{31}$$

Suppose the mth subaperture is steered to direction θ_0. The directional gain experienced by a scatterer at direction θ_i is given by [see (18)]

$$\zeta_{i,m} = \begin{cases} e^{-j2\pi(m-1)\Delta f_i} \frac{1-e^{-j2\pi L\Delta f_i}}{1-e^{-j2\pi\Delta f_i}}, & \theta_i \neq \theta_0 \\ L, & \theta_i = \theta_0 \end{cases} \tag{32}$$

where $\Delta f_i = f_i - f_0$ and $f_i = (\sin\theta_i)/2$ denotes the normalized spatial frequency. Clearly, for equal-sized subaperturing schemes, the directional gain offered by any of the M subapertures is identical in magnitude

$$|\zeta_{i,m_1}| = |\zeta_{i,m_2}|. \tag{33}$$

Fig. 2 depicts the magnitude of the directional gain for $N = 4$ antennas and $M = 2$ subapertures, which has two nulls at $\Delta f_i = \pm 1/3$. In general, with an N-element ULA and M transmit subapertures of an equal size $L = N - M + 1$, each of the transmit subaperture places a set of $L-1$ nulls at spatial frequencies Δf_i that are uniformly spaced between -0.5 and 0.5, excluding $\Delta f_i = 0$. Interferences located at these *fixed* directions are canceled by transmit subaperturing and beamforming. Interferences at other directions can be canceled by adaptive processing at the receiver side, which is discussed in Section IV.

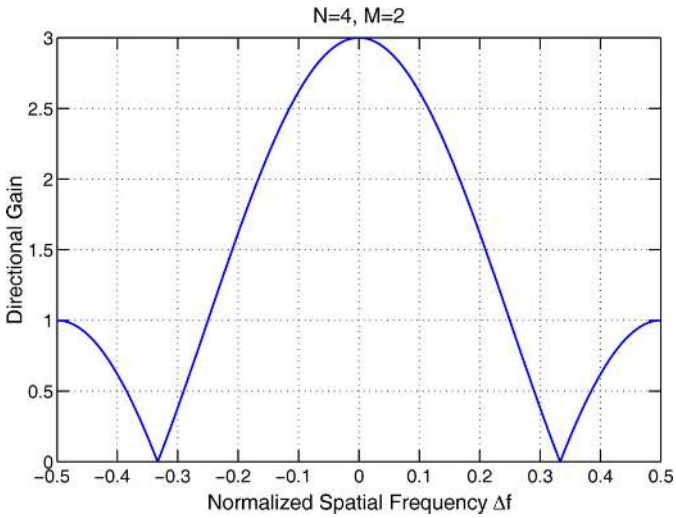

Fig. 2. Directional gain offered by transmit subaperturing/beamforming in the TS-MIMO radar with $N = 4$ antennas and $M = 2$ subapertures.

In this paper, we only consider untapered transmit beamforming for simplicity. Improved spatial selectivity and interference rejection can be achieved by applying a tapering window (e.g., Hamming window) along with our transmit subaperturing and beamforming scheme.

C. Discussions

The TS-MIMO radar can be considered as a hybrid system that offers some of the directional gain of the phased-array radar and also some of the interference rejection capability of the omni-MIMO radar. Since both attributes have a direct impact on the achievable performance in detecting a target in spatially distributed interference environments, it is of interest to examine how the TS-MIMO radar trades one attribute for the other. In the following, we discuss this and other related issues for the TS-MIMO radar.

1) Direction Gain Versus Interference Rejection: We examine the trade-off for the case considered in Section III-B, where ULAs are employed for both transmit and receive, by using the concept of *sum coarray*. The sum coarray was introduced in [15], [16] as a unifying tool for the understanding and analysis of transmit/receive array systems in radar, sonar, medical imaging, and other related applications. The sum coarray for the system described in Section III-B has $2N-1$ elements. Hence, there are a total of $2N-1$ DoFs for concentrating energy in the look direction and rejecting interference. It can be shown that the TS-MIMO system with M equal-sized subapertures has $N+M-1$ DoFs and, therefore, can adaptively cancel a maximum of $N+M-2$ interfering directions. This is because the TS-MIMO system trades off $N-M$ DoFs in the sum coarray to attain a directional gain of $N-M+1$, which leaves $(2N-1)-(N-M) = N+M-1$ DoFs. One DoF

is used to maintain a unity gain at the look direction, leaving $N + M - 2$ DoFs for interference rejection.

It follows from the above discussion that the TS-MIMO radar is effectively a *tunable* system, which not only subsumes the phased-array radar and the omni-MIMO radar as two extremal cases but also covers the full range of operation in between. At $M = 1$, it reduces to the phased-array radar, providing the maximum directional gain of N and an ability of rejecting up to $N - 1$ interferences. At $M = N$, it reduces to the omni-MIMO radar, capable of rejecting up to $2N - 2$ interferences but offering a unity directional gain. A unity directional gain is also considered as no directional gain since it is identically one at all directions. For every unity increase of the directional gain, the TS-MIMO radar gives away the ability to adaptively suppress one more interference.

The above analysis applies only to the ULA case. More general theories for arbitrary array configurations seem to be unavailable. However, computer simulation can be employed to assess the directional gain versus interference rejection trade-off in such cases.

2) Training Requirement: The interference-plus-noise covariance matrix $\mathbf{R}$ needs to be reliably estimated from training signals for adaptive processing (see Section IV). The amount of training required for reliable estimation is proportional to the dimension of the matched filter output (e.g., [13]), which is N_r, MN_r, and N_tN_r, respectively, for the phased-array, TS-MIMO and omni-MIMO radars. In typical radar operations, training signals are obtained using the radar returns from the range bins adjacent to the range bin under test (e.g., [14]), assuming that the environment is homogeneous. It is often necessary to reduce the training requirement, since as we seek more training by including range bins farther away from the test range bin for training purpose, the homogeneity assumption is more likely to be violated in a real-world environment. As we show in Section IV, the output SINR using an adaptively estimated covariance matrix is a function of K. When K is limited, we may have to switch from an omni-MIMO mode to a TS-MIMO mode with a suitable M, in order to achieve a target output SINR for reliable target detection.

3) Relation to Transmit Beamforming: In transmit beamforming, the waveforms transmitted from the antennas are correlated, determined by a correlation matrix $\mathbf{R}_w$. It is shown that $\mathbf{R}_w$ can be chosen to achieve or approximate a desired transmit beampattern [9]. A main objective of transmit beamforming is then to determine $\mathbf{R}_w$ and the corresponding signal waveforms for a given desired beampattern. This is in essence a constrained optimization problem that can only be solved numerically using some optimization routines [2], [9].

It is known that transmit beamforming includes the phased-array and omni-MIMO radars as special cases [9], when the signal correlation matrix is set to $\mathbf{R}_w = \mathbf{1}\mathbf{1}^T$ and $\mathbf{R}_w = \mathbf{I}$, respectively, where $\mathbf{1}$ denotes an all-one vector. The TS-MIMO radar can also be considered as a transmit beamforming scheme with some signal correlation matrix. Consider, for example, the ULA case involving $M = 2$ subapertures examined in Section III-B. The transmitted waveform across the entire array at a look angle θ_0 is the superposition of the signals sent by the two subapertures:

$$\begin{bmatrix} \mathbf{b}_1^*(\theta_0) \\ 0 \end{bmatrix} s_1(l) + \begin{bmatrix} 0 \\ \mathbf{b}_2^*(\theta_0) \end{bmatrix} s_2(l) \tag{34}$$

where the zero element in the vectors is due to the fact that there is one antenna excluded from each subaperture (which has a size of $N - 1$, while there are N antennas). Using the definition of the signal correlation matrix in [9] and recalling that $s_1(l)$ and $s_2(l)$ are orthogonal, we can readily show that $\mathbf{R}_w$ in this case is given by

$$\mathbf{R}_w = \frac{1}{L}\left\{ \begin{bmatrix} \mathbf{b}_1^*(\theta_0) \\ 0 \end{bmatrix} [\mathbf{b}_1^T(\theta_0) \quad 0] + \begin{bmatrix} 0 \\ \mathbf{b}_2^*(\theta_0) \end{bmatrix} [0 \quad \mathbf{b}_2^T(\theta_0)] \right\} \tag{35}$$

which is a rank-2 matrix as expected. The scaling factor $1/L$ is due to the assumption that $s_1(l)$ and $s_2(l)$ are normalized as in (22). In general, for an M-subaperture TS-MIMO, $\mathbf{R}_w$ is expected to have rank-M.

Despite its close relation to transmit beamforming, transmit subaperturing offers a unique perspective and tool for MIMO radar design and operation because it is simple, as no complex optimization is involved. Even more importantly, it can easily be "tuned" from one operating mode to another by changing the number and size of the subapertures, which provides a direct trade-off between processing gain and inference rejection ability of the system.

IV. Adaptive Beamforming and SINR Analysis

For comparison, we consider linear adaptive beamforming for the three radar systems, namely, the phased-array radar, omni-MIMO radar and TS-MIMO radar, and analyze their performance in terms of the output signal-to-interference-plus-noise ratio (SINR) of the adaptive beamformer. To simplify the discussion, we rewrite the output of the matched filter for the three systems as follows:

$$\begin{aligned} \mathbf{y} &= \alpha_0 \mathbf{a}(\theta_0) + \sum_i \alpha_i \mathbf{a}(\theta_i) + \mathbf{n} \\ &\triangleq \alpha_0 \mathbf{a}(\theta_0) + \mathbf{d} \end{aligned} \tag{36}$$

where the above equation may refer to any of (6), (12), and (26), and $\mathbf{d}$ denotes the *disturbance* or interference plus noise signal.

An adaptive beamformer is a linear spatial filter, expressed as a weight vector $\mathbf{w}$ with the same dimension as that of $\mathbf{y}$. A widely employed choice is the MDVR beamformer [11], [12]. The MVDR beamformer for a look angle θ_0 is given by

$$\mathbf{w}(\theta_0) = \frac{\hat{\mathbf{R}}^{-1}\mathbf{a}(\theta_0)}{\mathbf{a}^H(\theta_0)\hat{\mathbf{R}}^{-1}\mathbf{a}(\theta_0)} \tag{37}$$

where $\hat{\mathbf{R}}$ denotes an estimate of the covariance matrix $\mathbf{R}$ of the disturbance $\mathbf{d}$. Oftentimes the sample covariance matrix $\hat{\mathbf{R}}$ obtained via averaging over K training signal is employed

$$\hat{\mathbf{R}} = \frac{1}{K}\sum_{k=1}^{K} \mathbf{y}_k \mathbf{y}_k^H. \tag{38}$$

For typical radar operation, the training signals $\{\mathbf{y}_k\}_{k=1}^K$ are obtained using the radar returns from the range bins adjacent to the range bin of interest (e.g., [14]). The sample covariance matrix is also a consistent estimate of the true covariance matrix

$\mathbf{R}$ and converges to the latter as K increases. The beampattern is given by

$$P(\theta) = \left|\mathbf{a}^H(\theta)\mathbf{w}(\theta_0)\right|^2 \tag{39}$$

which is frequently used to show the performance of a beamformer in terms of its spatial resolution (i.e., mainbeam width) and interference rejection ability (sidelobe level and spectral nulls). We will examine the beampattern of the three radar systems in Section V.

Our focus here is the output SINR of the beamformer, which directly impacts the target detection performance in a spatially distributed interference environment. The beamformer output is given by

$$z = \mathbf{w}^H(\theta_0)\mathbf{y} = \alpha_0 + \mathbf{w}^H(\theta_0)\mathbf{d}. \tag{40}$$

Following the standard assumption that the target strength is deterministic whereas the disturbance $\mathbf{d}$ is stochastic with zero mean and covariance matrix $\mathbf{R}$ [14], the output SINR is

$$\gamma \triangleq \frac{|\alpha_0|^2}{E\{|\mathbf{w}^H(\theta_0)\mathbf{d}|^2\}} = \frac{|\alpha_0|^2}{\mathbf{w}^H(\theta_0)\mathbf{R}\mathbf{w}(\theta_0)}. \tag{41}$$

Substituting (37) into (41), we have

$$\gamma = \frac{|\alpha_0|^2\left[\mathbf{a}^H(\theta_0)\hat{\mathbf{R}}^{-1}\mathbf{a}(\theta_0)\right]^2}{\mathbf{a}^H(\theta_0)\hat{\mathbf{R}}^{-1}\mathbf{R}\hat{\mathbf{R}}^{-1}\mathbf{a}(\theta_0)}. \tag{42}$$

The output SINR is a random variable since it depends on $\hat{\mathbf{R}}$ which is random. Next, we examine the distribution of γ and related statistics under the standard assumption that disturbance signal $\mathbf{d}$ has a complex Gaussian distribution with zero mean and covariance matrix $\mathbf{R}$ [14]. In this case, the joint distribution of the entries of the sample covariance matrix $\hat{\mathbf{R}}$ is a complex Wishart distribution [17]. Using this knowledge, we can show that the output SINR (42) is a scaled Beta random variable. The proof, which is identical for all three radar systems, is skipped as it is similar to the one included in [18] on the distribution of the output SINR loss for the phased-array radar. Specifically, the probability density function (pdf) of γ in (42) is given by

$$\begin{aligned} f_\gamma(x) = &\frac{K!}{(N_{\text{syst}}-2)!(K+1-N_{\text{syst}})!\gamma_{\text{syst-max}}} \\ &\times\left(1-\frac{x}{\gamma_{\text{syst-max}}}\right)^{N_{\text{syst}}-2} \\ &\times\left(\frac{x}{\gamma_{\text{syst-max}}}\right)^{K+1-N_{\text{syst}}} \\ &0 \le x \le \gamma_{\text{syst-max}} \end{aligned} \tag{43}$$

where N_{syst} and $\gamma_{\text{syst-max}}$ are system specific parameters. Specifically, N_{syst} denotes the dimension of the matched-filter output $\mathbf{y}$ for the three systems, given by

$$N_{\text{pa}} = N_r \tag{44}$$

$$N_{\text{od}} = N_t N_r \tag{45}$$

$$N_{\text{ts}} = MN_r. \tag{46}$$

Meanwhile, $\gamma_{\text{syst-max}}$ denotes the maximum output SINR which is achieved when the disturbance covariance matrix $\mathbf{R}$ is known exactly

$$\gamma_{\text{pa}-\max} = |\alpha_0|^2\mathbf{a}_{\text{pa}}^H(\theta_0)\mathbf{R}_{\text{pa}}^{-1}\mathbf{a}_{\text{pa}}(\theta_0) \tag{47}$$

$$\gamma_{\text{od}-\max} = |\alpha_0|^2\mathbf{a}_{\text{od}}^H(\theta_0)\mathbf{R}_{\text{od}}^{-1}\mathbf{a}_{\text{od}}(\theta_0) \tag{48}$$

$$\gamma_{\text{ts-max}} = |\alpha_0|^2\mathbf{a}_{\text{ts}}^H(\theta_0)\mathbf{R}_{\text{ts}}^{-1}\mathbf{a}_{\text{ts}}(\theta_0). \tag{49}$$

We note that the directional gain for the phased-array and TS-MIMO radars is implicitly present in their steering vectors. In particular, we note that (47) can be expressed as [cf. (7)]

$$\gamma_{\text{pa}-\max} = N_t^2|\alpha_0|^2\mathbf{a}_r^H(\theta_0)\mathbf{R}_{\text{pa}}^{-1}\mathbf{a}_r(\theta_0) \tag{50}$$

where the SINR benefit due to coherent beamforming is shown as a constant N_t^2. Meanwhile, for the TS-MIMO radar, the steering vector $\mathbf{a}_{\text{ts}}(\theta_0)$ also scales with the directional gain [cf. (24) and (27)]. The SINR benefit becomes clearer for the example considered in Section III-B, for which (49) becomes

$$\gamma_{\text{ts-max}} = \kappa^2|\alpha_0|^2L^2\left[\mathbf{1}\otimes\mathbf{a}_r(\theta_0)\right]^H\mathbf{R}_{\text{ts}}^{-1}\left[\mathbf{1}\otimes\mathbf{a}_r(\theta_0)\right]^H. \tag{51}$$

The cumulative distribution function of the output SINR can be directly obtained from (43), which is given by

$$\begin{aligned} F_\gamma(x) = &\frac{K!}{(N_{\text{syst}}-2)!(K+1-N_{\text{syst}})!} \\ &\times B\left(\frac{x}{\gamma_{\text{syst}-\max}}; K+2-N_{\text{syst}}, N_{\text{syst}}-1\right) \end{aligned} \tag{52}$$

where

$$B(x;a,b) \triangleq \int_0^x t^{a-1}(1-t)^{b-1}dt \tag{53}$$

denotes the incomplete Beta function.

In addition, the first- and second-order moments of the output SINR can be computed from (43) in closed-form, which are convenient for comparing the three systems. Specifically, we have

$$E(\gamma) = \gamma_{\text{syst-max}}\frac{K+2-N_{\text{syst}}}{K+1} \tag{54}$$

$$E(\gamma^2) = \gamma_{\text{syst-max}}^2\frac{(K+2-N_{\text{syst}})(K+3-N_{\text{syst}})}{(K+2)(K+1)}. \tag{55}$$

It follows that the variance of the output SINR is given by

$$\text{var}(\gamma) = \gamma_{\text{syst-max}}^2\frac{(N_{\text{syst}}-1)(K+2-N_{\text{syst}})}{(K+2)(K+1)^2}. \tag{56}$$

An examination of (54) reveals the same well-known result of [18], that is, a total of $K \ge 2N_{\text{syst}} - 3$ i.i.d. training signals is needed to ensure that the mean output SINR of the adaptive beamformer is within 3 dB from its maximum achievable value. For sufficiently large N_{syst}, the above condition approximately reduces to $K \ge 2N_{\text{syst}}$.

V. Numerical Results

We now present numerical and simulation results to verify our analysis and compare the three radar systems, where similar to the example discussed in Section III-B, the transmitter

and receiver share a ULA of $N_t = N_r = N$ elements with half-wavelength inter-element separation. For the TS-MIMO radar, a total of M transmit subapertures with maximum overlapping are formed, as discussed in Section III-B.[1] For all three systems, a target is located at 0.1 cycles per wavelength (in normalized spatial frequency) and multiple interferences are at other locations. The average power for each interference is 1 and the noise variance is $\sigma_n^2 = 0.01$. The target power is either $|\alpha_0|^2 = 1$ or varied over a range of values as specified. In the following, we consider several test cases with different values of N, M, and N_i, where the latter denotes the number of interferences. All computer simulation results are based on 200 independent Monte Carlo runs.

A. Test Case 1: $N = 4$ and $N_i = 3$

The first case is one where the number of interferences can be handled by all three radar systems. Specifically, there are $N = 4$ transmit/receive antennas and $N_i = 3$ interferences at $(-0.41, -0.21, -0.01)$ in normalized spatial frequencies. The TS-MIMO radar forms $M = 2$ transmit subapertures, each consisting of three antenna elements and maximally overlapping with the other subaperture as explained in Section III-B. The adaptive MVDR beamformer is considered for the three radar systems, using $K = 2N^2 = 32$ training signals[2] to estimate the interference-plus-noise covariance matrix $\mathbf{R}$. The beamformer is steered toward the target direction and under this condition, we examine the output SINR and beampattern of the beamformer.

Fig. 3(a) and (b) depicts the mean and, respectively, standard deviation (STD) of the output SINR obtained by using (54) and (56) and by simulation. The analytical and simulation results are observed to agree with each other. We note that the STD value for a given target power is notably less than the corresponding mean value (by over 10 dB for the phased-array and TS-MIMO radars), which indicates that fluctuation in the output SINR is relatively small. Henceforth, we will skip any further STD results. The mean output SINR shows that all three radar systems work well, due to effective cancellation of the interferences. Although their performances are similar, the phased-array radar is noticed to outperform the omni-MIMO radar by 2.5 dB, due to a directional gain. Interestingly, the TS-MIMO radar achieves the best performance, yielding a gain of about 1.5 dB over the phased-array radar. This is due to its stronger interference mitigation ability over the phased-array radar. It is noted that at $N_i = 3$, the phased-array radar with $N = 4$ antennas reaches its maximum number of interferences that can be handled, whereas the TS-MIMO radar has more room. The beampatterns of the adaptive MVDR beamformers for the three systems are shown in Fig. 3(c). It is seen that all three beamformers adaptively placed spectral nulls at the interference directions.

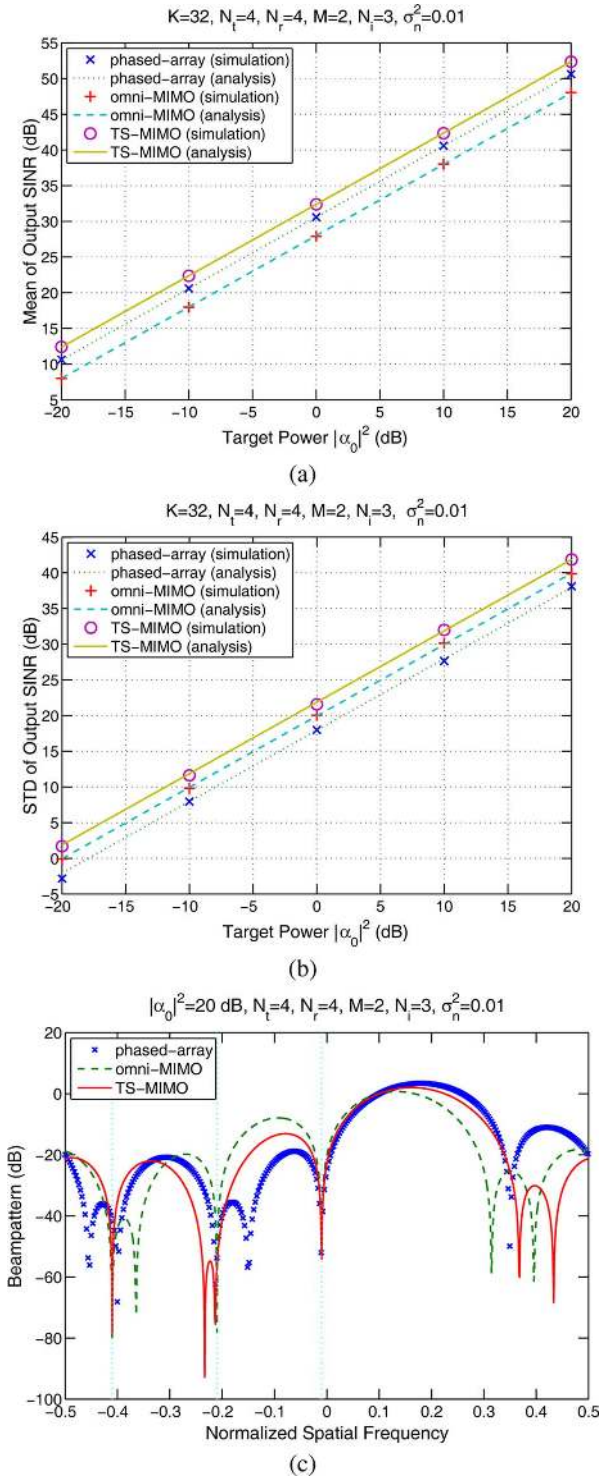

Fig. 3. (a) Mean and (b) standard deviation of the output SINR, and (c) beampatterns of the beamformers for the phased-array, omni-MIMO and TS-MIMO ($M = 2$ subapertures) radars with $N = 4$ antennas, $K = 32$ training signals, and $N_i = 3$ interferences.

B. Test Case 2: $N = 4$ and $N_i = 4$

We now consider a case with $N_i = 4$ interferences located at $(-0.41, \quad -0.21, \quad 0.21, \quad 0.41)$ in normalized spatial frequencies. The TS-MIMO radar uses $M = 2$ transmit subapertures, configured identically as in the previous example. The mean output SINR and beampatterns are shown in Fig. 4(a) and (b), respectively. In the current case, the phased-array radar becomes the worst performer. It cannot effectively cancel all $N_i = 4$ interferences, as seen from its

[1]Equivalently, comparisons reported next can be considered to be among different modes of the TS-MIMO radar, since it reduces to the phased-array and omni-MIMO radars by setting $M = 1$ and, respectively, $M = N$. For simplicity, a TS-MIMO radar here only refers to the case $1 < M < N$.

[2]This ensures that the omni-MIMO radar, which requires more training signals than the other two systems to converge, works properly; see discussions following (56).

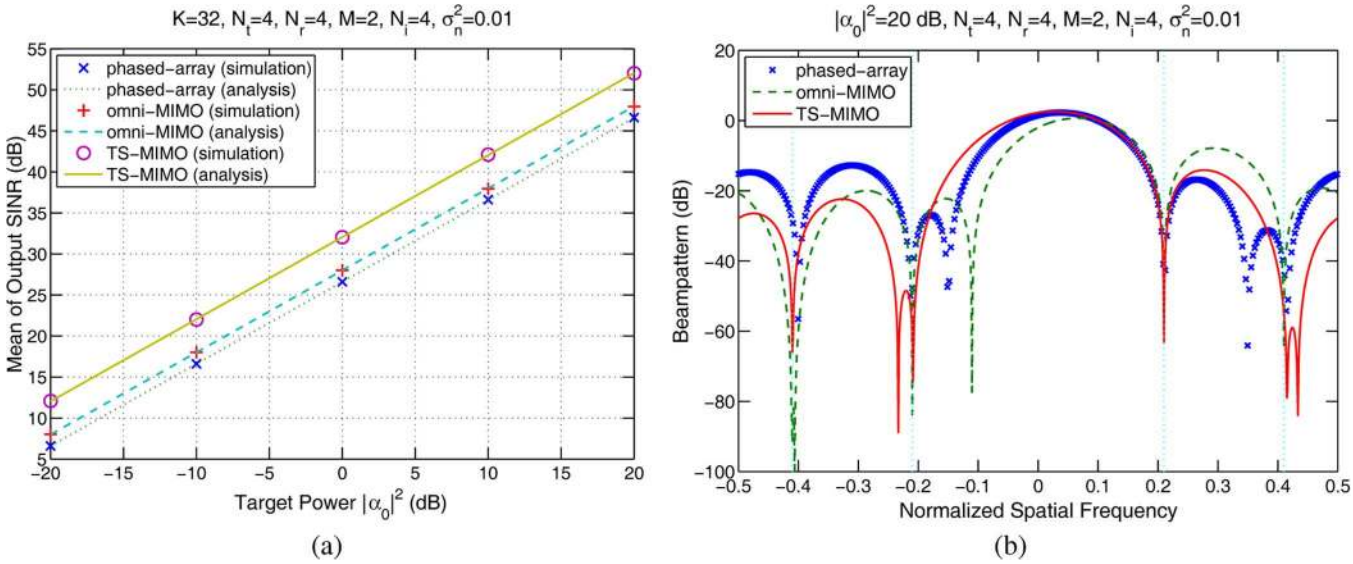

Fig. 4. (a) Mean of the output SINR and (b) beampatterns of the beamformers for the phased-array, omni-MIMO, and TS-MIMO ($M = 2$ subapertures) radars with $N = 4$ antennas, $K = 32$ training signals, and $N_i = 4$ interferences.

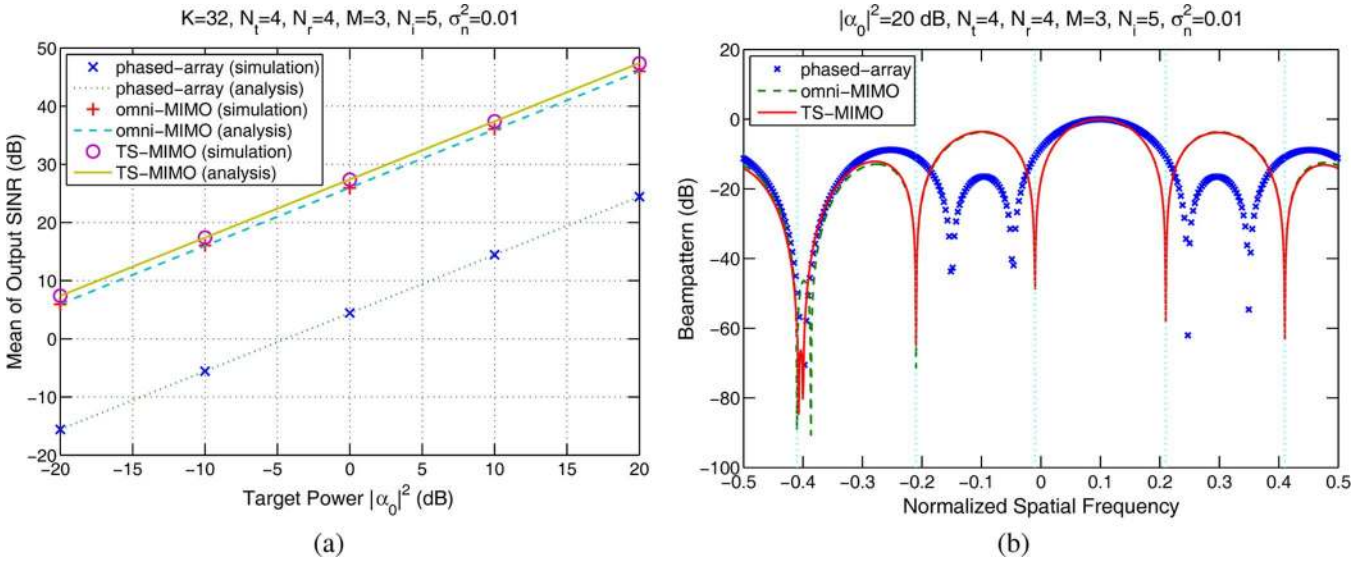

Fig. 5. (a) Mean of the output SINR and (b) beampatterns of the beamformers for the phased-array, omni-MIMO, and TS-MIMO ($M = 3$ subapertures) radars with $N = 4$ antennas, $K = 32$ training signals, and $N_i = 5$ interferences.

beampattern in Fig. 4(b). Meanwhile, the TS-MIMO is again the best scheme in terms of the output SINR, yielding a performance advantage of about 4 dB over the omni-MIMO radar.

C. *Test Case 3:* $N = 4$ *and* $N_i = 5$

We next increase the number of interferences to $N_i = 5$ located at normalized spatial frequencies (-0.41, -0.21, -0.01, 0.21, 0.41). As discussed in Section III-C, the TS-MIMO radar in the current case needs to increase to $M = 3$ transmit subapertures to mitigate all five interferences, by reducing the directional gain by 1. Each of the three subaperture consists of two adjacent antenna elements and overlaps with another subaperture by one element. The mean output SINR and beampatterns are shown in Fig. 5(a) and (b), respectively. The phased-array radar is much worse than the other two in this case. Its beampattern reveals that it misses all but one interference (located at spatial frequency -0.41). In contrast, the MIMO radars can suppress all five interferences, as indicated by their beampatterns. The TS-MIMO radar, however, has a small advantage of about 1.4 dB, due to its directional gain, over the omni-MIMO radar. It should be noted that while the omni-MIMO radar for the current setup can handle up to six interferences, the TS-MIMO radar with a subaperture size of $L = 2$ can adaptively suppress up to five interferences, due to the trade-off between directional gain and interference rejection as discussed in Section III-C.

D. *Test Case 4:* $N = 7$ *and* $N_i = 7$

In the last test case, we consider a larger array and show the directional gain provided by the TS-MIMO can be quite significant. Specifically, suppose there are $N = 7$ antennas, $N_i = 7$ interferences located at spatial frequencies (-0.41, -0.31, -0.21, -0.01, 0.21, 0.41), and $K = 2N^2 = 98$ training signals are used for adaptive processing. The TS-MIMO employs $M = 2$ transmit subapertures with maximum overlapping.

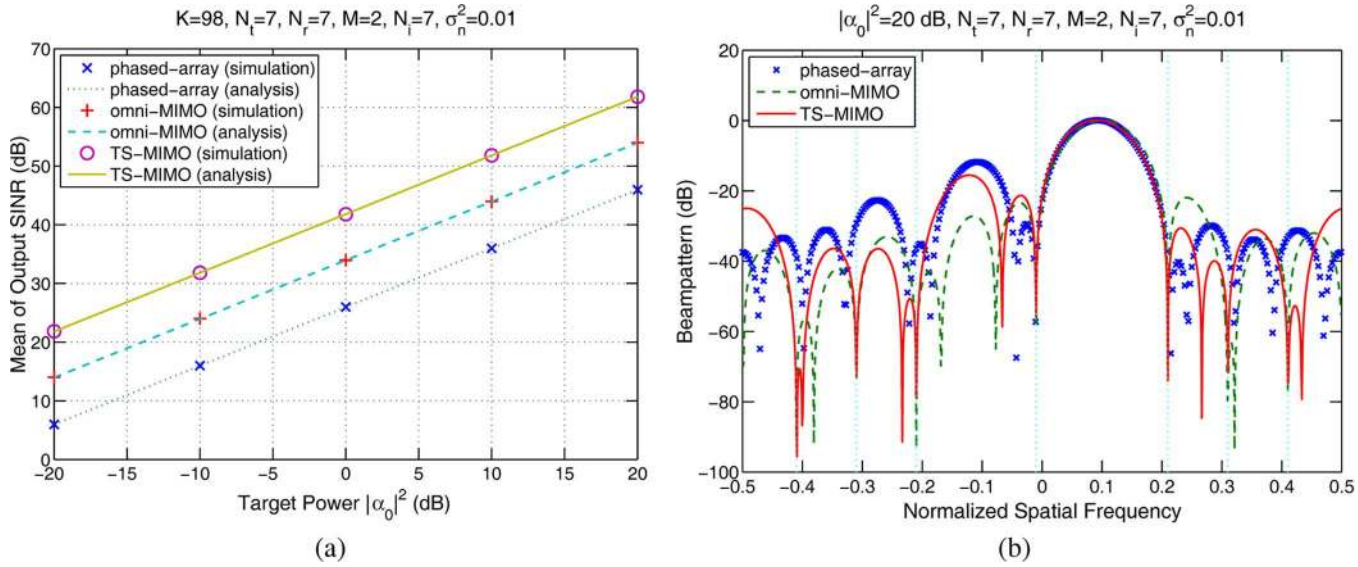

Fig. 6. (a) Mean of the output SINR and (b) beampatterns of the beamformers for the phased-array, omni-MIMO, and TS-MIMO ($M = 2$ subapertures) radars with $N = 7$ antennas, $K = 98$ training signals, and $N_i = 7$ interferences.

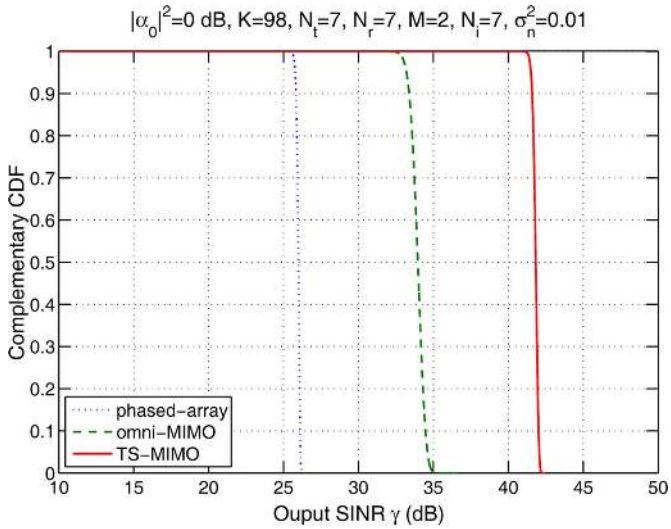

Fig. 7. Complementary CDF of the beamformer output SINR for the phased-array, omni-MIMO, and TS-MIMO ($M = 2$ subapertures) radars with $K = 98$ training signals and $N_i = 7$ interferences.

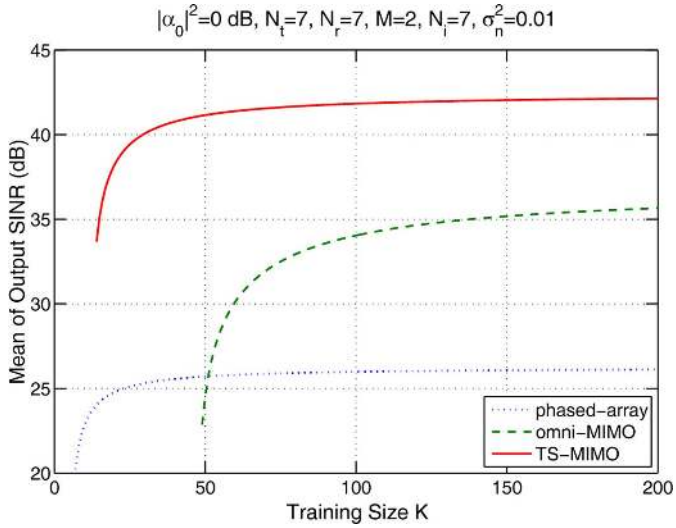

Fig. 8. Convergence rate of the mean output SINR for the phased-array, omni-MIMO and TS-MIMO ($M = 2$ subapertures) radars with $N_i = 7$ interferences.

Fig. 6(a) and (b) shows the mean output SINR and beampatterns, respectively. It is seen that all seven interferences are effectively canceled by the two MIMO radars. However, in terms of the output SINR, the TS-MIMO radar enjoys an impressive gain of almost 8 dB over the omni-MIMO radar.

Fig. 7 depicts the complementary CDF of the output SINR for the three systems when $|\alpha_0|^2 = 1$ and other parameters are the same as before. The complementary CDF is defined as $1 - F_\gamma(x)$, where $F_\gamma(x)$ is shown in (52). We use the complementary CDF instead of the CDF as the former is convenient to show that the maximum output SINR, achieved when $\mathbf{R}$ is known or equivalently $K = \infty$, for the three systems. Specifically, the maximum output SINRs, from (47)–(49), are 26.3 dB, 36.8 dB, and 42.4 dB for the phased-array, omni-MIMO and TS-MIMO radars, respectively, also shown in the figure. We see that compared with the omni-MIMO radar, transmit subaperturing offers an SINR gain of 5.6 dB in terms of the maximum output SINR. At 90 percentile (i.e., 0.9 for the complementary CDF), the gain of the TS-MIMO over the omni-MIMO radar is about 8.2 dB.

Finally, we consider the convergence rate of the adaptive MVDR beamformers for the three radar systems. Fig. 8 shows the mean of the output SINR for varying K, the number of training signals used to estimate the sample covariance matrix $\hat{\mathbf{R}}$. Since $\hat{\mathbf{R}}$ has to be full rank, the minimum K is the dimension of the matched-filter output, which is 7, 14, and 49, respectively, for the phased-array, omni-MIMO and TS-MIMO radars. We see that all three systems converge to their maximum output SINR as K increases, with the convergence rate of the phased-array radar being the fastest due to its smallest data dimension.

VI. Conclusion

We proposed a transmit subaperturing approach for MIMO radars. The resulting TS-MIMO radar is a tunable system that offers a continuum of operating modes including the phased-array and omni-MIMO modes as two extremes. The TS-MIMO system was examined in an interference and training limited environment, where analytical tools were derived to show the interplay among the number/size of transmit subapertures, number of training signals, and target/interference powers, and how they affect the output SINR. The tools are particularly useful for applications where the primary goal is target detection in an interference and training limited environment, frequently encountered in the real world. Our numerical results show that it may be beneficial, and sometimes even necessary, to properly select the operating mode of the TS-MIMO system with a suitable subaperture configuration (in terms of the size/number of subapertures) so that the output SINR is maximized for reliable target detection. Blindly resorting to the extremal phased-array mode or the omni-MIMO mode may result in unnecessary penalty in the output SINR.

It should be noted that our focus of the output SINR was mainly motivated from a target detection perspective, where it is an important performance metric. In other applications, e.g., surveillance of an unknown field, the omni-MIMO mode is likely most useful due to its broad transmit spatial patterns, which can achieve a higher search or scan rate.

Acknowledgment

The authors would like to thank the anonymous reviewers for their helpful and constructive comments that led to a significant improvement of the manuscript. They are particularly indebted to one reviewer who suggested the theory of sum coarray for the analysis of the TS-MIMO system.

References

[1] M. I. Skolnik, *Introduction to Radar Systems*, 3rd ed. New York: McGraw-Hill, 2001.

[2] J. Li and P. Stoica, "MIMO radar with colocated antennas," *IEEE Signal Process. Mag.*, vol. 24, no. 5, pp. 106–114, Sep. 2007.

[3] A. M. Haimovich, R. S. Blum, and L. J. Cimini, "MIMO radar with widely separated antennas," *IEEE Signal Process. Mag.*, vol. 25, no. 1, pp. 116–129, Jan. 2008.

[4] E. Fishler, A. M. Haimovich, R. S. Blum, L. J. Cimini, Jr, D. Chizhik, and R. A. Valenzuela, "Spatial diversity in radars—Models and detection performance," *IEEE Trans. Signal Process.*, vol. 54, no. 3, pp. 823–838, Mar. 2006.

[5] D. W. Bliss and K. W. Forsythe, "Multiple-input multiple-output (MIMO) radar and imaging: Degrees of freedom and resolution," in *Proc. 37th Asilomar Conf. Signals, Syst., Comput.*, Pacific Grove, CA, Nov. 2003, vol. 1, pp. 54–59.

[6] J. Li, P. Stoica, L. Xu, and W. Roberts, "On parameter identifiability of MIMO radar," *IEEE Signal Process. Lett.*, vol. 14, no. 12, pp. 968–971, Dec. 2007.

[7] L. Xu, J. Li, and P. Stoica, "Target detection and parameter estimation for MIMO radar systems," *IEEE Trans. Aerosp. Electron. Syst.*, vol. 44, no. 3, pp. 927–939, Jul. 2008.

[8] F. C. Robey, S. Coutts, D. Weikle, J. C. McHarg, and K. Cuomo, "MIMO radar theory and experimental results," in *Proc. 38th Asilomar Conf. Signals, Syst., Comput.*, Pacific Grove, CA, Nov. 2004, vol. 1, pp. 300–304.

[9] D. R. Fuhrmann and G. S. Antonio, "Transmit beamforming for MIMO radar systems using signal cross-correlation," *IEEE Trans. Aerosp. Electron. Syst.*, vol. 44, no. 1, pp. 171–186, Jan. 2008.

[10] P. Stoica, J. Li, and Y. Xie, "On probing signal design for MIMO radar," *IEEE Trans. Signal Process.*, vol. 55, no. 8, pp. 4151–4161, Aug. 2007.

[11] B. D. Van Veen and K. M. Buckley, "Beamforming: A versatile approach to spatial filtering," *IEEE Acoust., Speech, Signal Process. Mag.*, vol. 5, no. 2, pp. 4–24, Apr. 1988.

[12] J. Capon, "High resolution frequency-wavenumber spectrum analysis," *Proc. IEEE*, vol. 57, no. 8, pp. 1408–1418, Aug. 1969.

[13] P. Stoica and R. L. Moses, *Introduction to Spectral Analysis*. Upper Saddle River, NJ: Prentice-Hall, 1997.

[14] J. Ward, "Space–time adaptive processing for airborne radar," Lincoln Laboratory, MIT, 1994, Tech. Rep. 1015.

[15] R. T. Hoctor and S. A. Kassam, "The unifying role of the coarray in aperture synthesis for coherent and incoherent imaging," *Proc. IEEE*, vol. 78, no. 4, pp. 735–752, Apr. 1990.

[16] R. T. Hoctor and S. A. Kassam, "High resolution coherent source location using transmit/receive arrays," *IEEE Trans. Image Process.*, vol. 1, pp. 88–100, Jan. 1992.

[17] N. R. Goodman, "Statistical analysis based on a certain multivariate complex Gaussian distribution," *Ann. Math. Statist.*, vol. 34, no. 1, pp. 152–177, Mar. 1963.

[18] I. S. Reed, J. D. Mallett, and L. E. Brennan, "Rapid convergence rate in adaptive arrays," *IEEE Trans. Aerosp. Electron. Syst.*, vol. AES-10, no. 6, pp. 853–863, Nov. 1974.

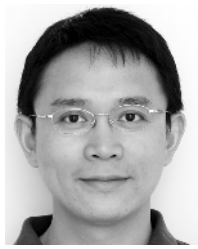

Hongbin Li (M'99–SM'08) received the B.S. and M.S. degrees from the University of Electronic Science and Technology of China, Chengdu, in 1991 and 1994, respectively, and the Ph.D. degree from the University of Florida, Gainesville, in 1999, all in electrical engineering.

From July 1996 to May 1999, he was a Research Assistant in the Department of Electrical and Computer Engineering, University of Florida. He was a Summer Visiting Faculty Member at the Air Force Research Laboratory in the summers of 2003, 2004, and 2009. Since July 1999, he has been with the Department of Electrical and Computer Engineering, Stevens Institute of Technology, Hoboken, NJ, where he is an Associate Professor. His current research interests include statistical signal processing, wireless communications, and radars.

Dr. Li is a member of Tau Beta Pi and Phi Kappa Phi. He received the Harvey N. Davis Teaching Award in 2003 and the Jess H. Davis Memorial Award for excellence in research in 2001 from Stevens Institute of Technology, and the Sigma Xi Graduate Research Award from the University of Florida in 1999. He is a member of the Sensor Array and Multichannel (SAM) Technical Committee of the IEEE Signal Processing Society. He is/has been an Editor or Associate Editor for the IEEE Transactions on Wireless Communications, IEEE Signal Processing Letters, and the IEEE Transactions on Signal Processing, and a Guest Editor for the *EURASIP Journal on Applied Signal Processing*.

Braham Himed (S'88–M'90–SM'01–F'07) was born in Algiers, Algeria. He received the B.S. degree in electrical engineering from Ecole Nationale Polytechnique of Algiers in 1984, and the M.S. and Ph.D. degrees in electrical engineering from Syracuse University, Syracuse, NY, in 1987 and 1990, respectively.

He is currently a Principal Electronics Engineer with the Air Force Research Laboratory, Sensors Directorate, Radar Signal Processing Branch, Dayton, OH. His research interests include detection, estimation, multichannel adaptive signal processing, time series analyses, array processing, space–time adaptive processing, hot clutter mitigation, airborne, and spaceborne radar, over the horizon radar, and below-ground sensing.

Dr. Himed is the recipient of the 2001 IEEE region award for his work on bistatic radar systems, algorithm development, and phenomenology. He is a member of the Aerospace and Electronic Systems Radar Systems Panel.